

Aluminum on the Si(100) surface: Growth of the first monolayer

J. Nogami

Department of Physics and Laboratory for Surface Studies, University of Wisconsin-Milwaukee, Milwaukee, Wisconsin 53201

A. A. Baski and C. F. Quate

Department of Applied Physics, Stanford University, Stanford, California 94305

(Received 9 April 1991)

Scanning tunneling microscopy was used to study the growth of the first monolayer (ML) of Al on the Si(100) surface at room temperature (up to 100°C). The Al forms rows of adsorbed dimers that run perpendicular to the underlying Si dimer rows. As the coverage is increased, the metal configuration evolves from isolated rows, to areas of local 2×3 and 2×2 structure, to a surface entirely terminated by a 2×2 array of Al dimers at 0.5 ML. Deposition of more than 0.5 ML results in the growth of three-dimensional Al clusters on the 2×2 surface. Electronic-structure effects are illustrated, and two alternative bonding sites for the Al adatom dimers are suggested.

We have studied the growth of the first monolayer (ML) of Al on Si(100) with scanning tunneling microscopy (STM). We report here on the behavior between room temperature and 100°C, a regime in which the evolution of the surface is relatively simple, and analogous to that seen for Ga and In on Si(100). Our previous STM work on Ga and In concentrated on the behavior up to 0.5 ML.¹⁻⁴ Here we show how Al growth changes as the coverage exceeds 0.5 ML. We also discuss effects of the electronic structure on the STM images, and what implications they have on interpretation of the measurements.

Of the three group-III metal/Si(100) systems that we have studied, Al/Si(100) is the least well characterized in prior work. The only recent experimental work is a study by low-energy electron diffraction (LEED) which detected several ordered phases at metal coverages up to 1 ML.⁵ In addition, total-energy calculations have been done for several bonding arrangements of Al and Ga on Si(100) which are both consistent with previous experimental data for Ga on Si(100).⁶ The models that have been proposed for Al on Si(100) are mostly derived by analogy with Ga and In, metals for which more extensive measurements have been made.⁷⁻⁹

Figure 1 is a set of three diagrams showing the ordered phases that arise when group-III metals are deposited on the Si(100) surface.^{5,7,8} These diagrams are a summary of LEED and RHEED (reflection high-energy electron diffraction) data taken for a range of substrate temperatures and for metal coverages up to 1 ML. The labels marked by ovals indicate regions of the phase diagrams that have been investigated in this and previous STM studies. Although these systems behave differently at higher temperatures, their behavior up to 150°C is basically the same. A gradual breaking up of the clean surface 2×1 order occurs with metal deposition, followed by the establishment of a 2×2 phase at 0.5 ML. Ga is slightly different in that there is an intermediate 2×3 phase at ≈ 0.3 ML, but the degree to which the 2×3 is ordered enough to appear in LEED depends strongly on the substrate temperature. Our own measurements have shown that for all three metals, only the 2×2 phase at 0.5 ML is seen in LEED for deposition of up to one monolayer at

room temperature (below 50°C).

All sample preparation and measurements were carried out in an ultrahigh vacuum (UHV) system with facilities for sample heating, metal deposition, and characterization by LEED and STM.¹⁰ Si(100) samples were cut from commercial wafer stock, chemically cleaned immediately before introduction to vacuum, and then flashed briefly in UHV at 1150°C. Aluminum was evaporated from a heated tungsten filament onto substrates at or below 100°C. Because of the proximity of the quartz crystal microbalance to the evaporator, heating affected the calibration of the thickness monitor and made it difficult to determine the absolute rate of metal deposition. However,

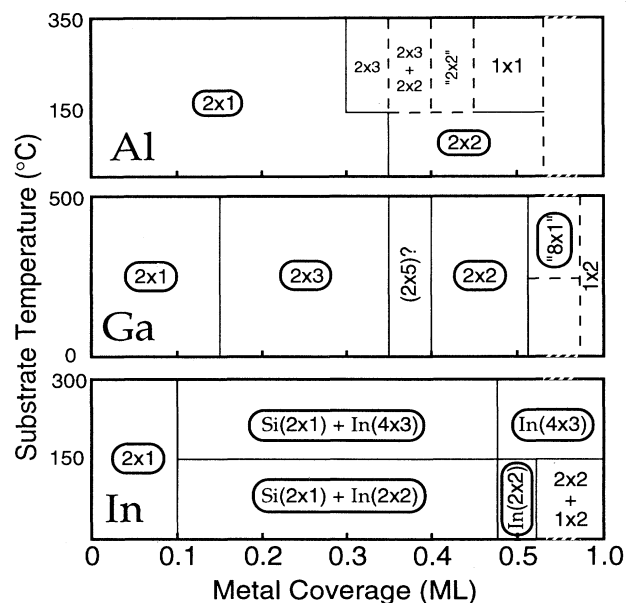


FIG. 1. Phase diagrams for the different reconstructions of Si(100) induced by group-III metals, as seen by electron diffraction. Phases marked by ovals indicate those seen in this and previous STM studies. The temperature scale is different for each of the panels, and the region of metal coverage between 0.5 and 1.0 ML has been compressed.

relative coverages could be determined from both the power to the evaporator filament and the deposition time. Absolute coverages were calibrated by determining the coverage at which the 2×2 LEED pattern appeared, which was known to be 0.5 ML. At coverages below this point, a more accurate determination was made by counting the density of metal-related features on the surface seen in the STM images, assuming the same correspondence between feature density and metal coverage as seen in the analogous Ga/Si(100) and In/Si(100) systems. Coverages are given in monolayers, with 1 ML defined as the Si atom density on the Si(100) surface ($1 \text{ ML} = 6.8 \times 10^{14} \text{ cm}^{-2}$). All STM imaging was done at room temperature.

The evolution of the surface with Al coverage up to 0.5 ML is shown in Fig. 2. The sequence of coverages is 0.1, 0.2, 0.25, and 0.4 ML for Figs. 2(a)–2(d), respectively. Figure 2(a) is a filled electronic state image, taken while tunneling out of the sample. At this low coverage, most of the features in the STM image are due to the clean surface. Rows of Si dimers are seen running diagonally from the upper left-hand to the lower right-hand corners. Deposition of Al results in long lines, roughly one unit cell wide, running perpendicular to the Si dimer rows. A few of these rows are seen cutting across the central part of the image. The remaining images in Fig. 2 are of the empty states. As will be discussed later, the Al-related features are much more prominent in the empty rather than in the filled state images. Also, a two-unit cell ($2a$, where $a = a_0/\sqrt{2} = 3.84 \text{ \AA}$) periodicity along each row is more apparent in the empty states. However, the principle features are the same in either bias: the Al forms long rows running perpendicular to the Si dimer rows on the surface. As the coverage is increased, the spacing between these rows decreases and preferred spacings become apparent. At 0.3 ML [Fig. 2(c)], many of the rows are either $2a$ or $3a$ apart. As the coverage approaches 0.5 ML [Fig. 2(d)], most of the rows are spaced $2a$ apart. The inter-row spacing of $2a$, in conjunction with the $2a$ period-

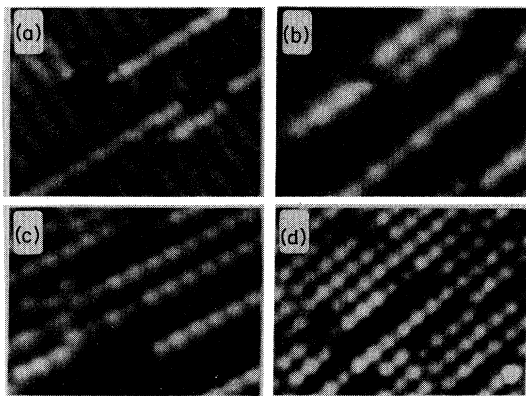


FIG. 2. Four images showing the coverage evolution of the surface below 0.5 ML of Al. The sequence of coverages is 0.1, 0.2, 0.25, and 0.4 ML for Figs. 2(a)–2(d), respectively. Figure 2(a) is a filled state image. The remaining three figures are empty state images.

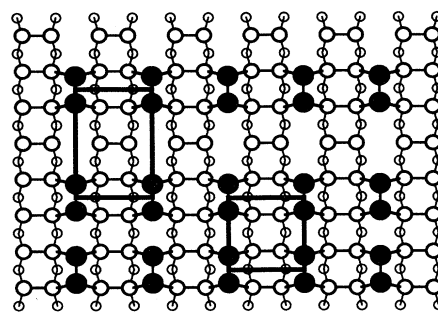


FIG. 3. A diagram showing the formation of 2×3 and 2×2 phases according to the standard metal dimer model. Al dimers are shown in black.

icity along each row, results in 2×2 two-dimensional ordering at 0.5 ML.

STM images of both Ga and In on Si(100) show the same room-temperature evolution of the surface for metal coverages up to 0.5 ML.^{2,4} For both of these metals, a comparison between the density of the metal rows and the nominal metal coverage showed that each row corresponds to one metal atom per Si 1×1 unit cell. Given that each metal row consists of maxima spaced $2a$ apart, each of these maxima should then be associated with two metal atoms. This assignment of two metal atoms to each maximum, and the position of each maxima with respect to the adjacent Si dimers, both support the model shown in Fig. 3. In this diagram, the metal atoms are adsorbed on the surface as dimers. The dimers are arranged in rows, as seen in the STM images. When these rows are $3a$ ($2a$) apart, local areas of 2×3 (2×2) order are formed. This model has been invoked previously to explain the 2×3 and 2×2 phases for Al, Ga, and In on Si(100).^{5,7,8} The 2×2 arrangement at 0.5 ML is the densest possible packing of rows in this structure. When the Al dimers are packed in the 2×2 phase, all dangling bonds in the underlying Si surface are terminated and all Al atoms are bonded to three neighbors.

Since it is not possible to place any more Al atoms on the surface in the same bonding arrangement once the 2×2 phase is formed, one suspects that the behavior of the Al will change above 0.5 ML. Figure 4 shows the surface after the deposition of approximately 0.6 ML of Al. The

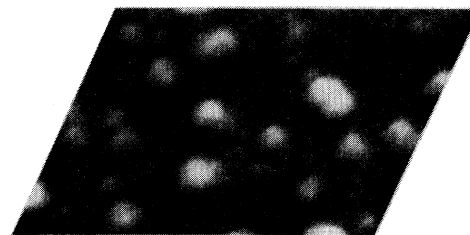


FIG. 4. An image of 0.6 ML of Al on the surface. The square array covering most of the surface is the 2×2 phase. Deposition of more than 0.5-ML Al results in the growth of Al clusters on the surface, which appear as bright irregular shapes in this topograph.

square array of dots covering most of the surface corresponds to the 2×2 phase. On top of this layer, the Al forms three-dimensional (3D) clusters. These clusters are visible as irregular white shapes in the image. At this coverage, the clusters are still relatively small with an average height of 3–5 Å above the 2×2 surface. Further metal deposition results in the growth of these clusters, eventually making STM imaging difficult because of both increased surface roughness, and instability of the metal in the clusters under the influence of the STM tip.

This type of growth behavior could be described as a Stranski-Krastanov (SK) mode. However, it is slightly unusual in that the transition to 3D growth occurs before the completion of the first monolayer of metal deposition. Partially, this is a matter of definition, since the 2×2 surface at 0.5 ML is complete in the sense that it has essentially no occupied surface dangling bonds. Two previous non-STM studies of In and Ga on Si(100) report a transition to 3D cluster growth only at or above 1 ML, even though these metals have a similar 2×2 phase at 0.5 ML.^{7,9} We have produced a surface free of 3D metal clusters between 0.5 and 1 ML coverage in the case of Ga/Si(100), but only by annealing the surface.² Annealing above 0.5 ML of Al on the surface disrupted the 2×2 order without eliminating the 3D clusters.

With the identification of the maxima in the STM images as Al dimers, it should be noted that there is never any indication of Al adsorbing as single atoms or in other bonding arrangements for even the lowest coverages. Between room temperature and 100°C, the Al is always mobile enough to form the dimer rows, although there is a tendency to form shorter, more numerous rows at lower substrate temperatures for a given metal coverage.

We now examine the bias dependence of the images below 0.5 ML more closely. Figure 5 shows a dual-bias image of a surface showing a mixture of 2×3 and 2×2 order. The two images were taken in parallel in order to retain their spatial registration. In the empty state image [Fig. 5(a)], the Al-related features appear as bright rows of $2a$ spaced maxima, as in Figs. 2(b)–2(d) and Fig. 4. The filled state image [Fig. 5(b)] is qualitatively the same

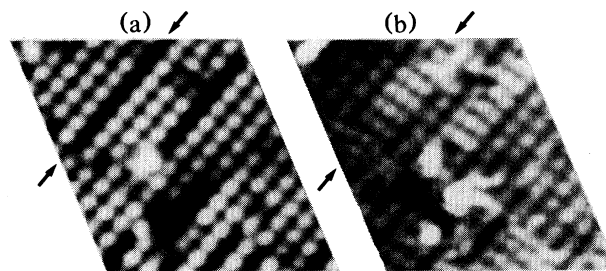


FIG. 5. A pair of images of the surface at 0.4 ML, taken in parallel at -2 -V and $+2$ -V tip bias, showing the (a) empty and the (b) filled states of the surface. A pair of arrows indicates a single row of 2×3 unit cells in both images.

in its arrangement of maxima, aside from considerably less corrugation than in the empty states. There is a more significant difference between the two images in regions where the dimer rows are spaced $3a$ apart. One of the rows of 2×3 unit cells is indicated by a pair of arrows in both images. The filled state image shows an additional row of maxima in the center of the 2×3 unit cells. In addition, there is a 180° phase shift of the maxima along each row between the filled and empty states.

The registration of the maxima in both the empty (solid circles) and the filled (dashed circles) states is shown in Fig. 6. Adjacent rows of 2×3 and 2×2 unit cells are shown in this diagram. The model in Fig. 3 places the metal dimers in the positions corresponding to the empty state maxima which lie in the trenches between the underlying Si dimer rows. The placement of the dimers in the positions of the empty, rather than the filled, state maxima is justified in view of the resultant bonding configuration of the metal dimers. In the configuration shown in Fig. 3, each trivalent metal atom is bonded to three neighbors, leaving essentially no occupancy of the dangling-bond state that points up away from the surface. This results in a strong maximum in the empty state density above each metal dimer. It is more difficult to explain all

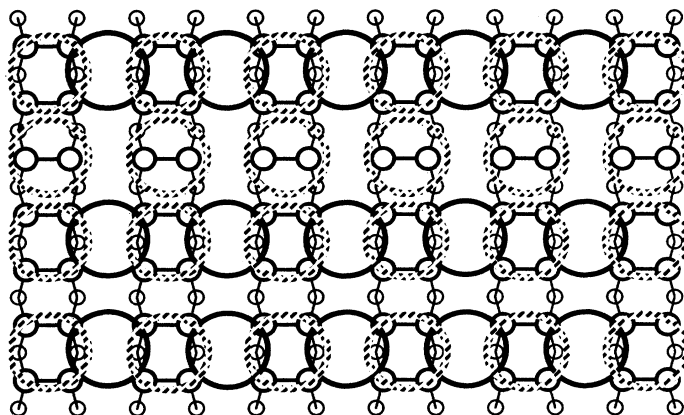


FIG. 6. A diagram showing the registration of the features seen in Fig. 5 with respect to the underlying Si dimers. The maxima in the empty (filled) states are indicated by a heavy solid (dashed) circular outline.

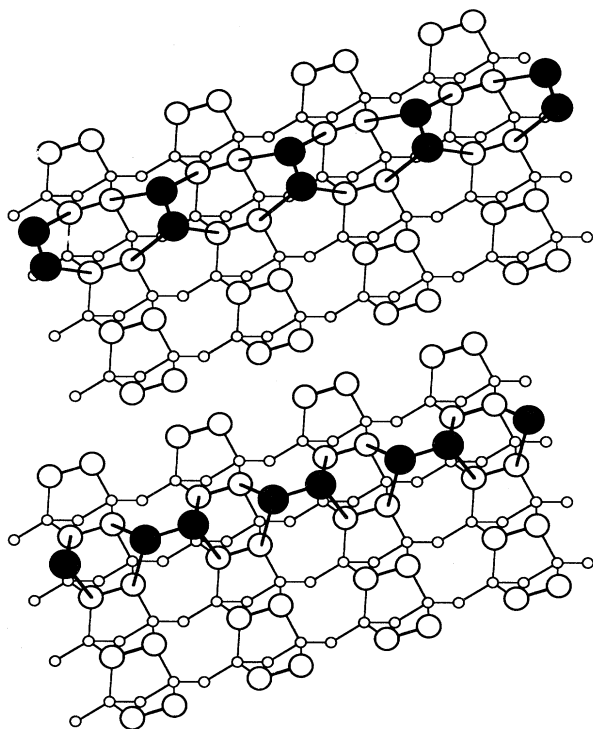


FIG. 7. Two possible bonding arrangements of the Al dimers on the surface. The Al dimers are positioned either perpendicular (upper panel) or parallel (lower panel) to the underlying Si dimers.

of the features of the filled state charge distribution seen in the images without a detailed calculation. However, the following points can be made. Filled state images show that isolated Al dimer rows are essentially at the same apparent "height" as the surrounding Si dimers [Fig. 2(a)]. Given this fact, it is possible that the "addi-

tional" maximum located in the center of each 2×3 unit cell could be the Si dimer lying midway between the Al dimer rows. The maxima lying "between" the Al dimers (within each row) could be a combination of the state density above Si dimers under the Al dimers, as well as that above the Al-Si bonds themselves. Calculations on the Al/Si(100) 2×2 structure show that there is a significant redistribution of charge density around each Al dimer.⁶

One final point needs to be addressed: is the dimer configuration shown in Fig. 3 the only possibility? There are actually two configurations in which Al dimers could be placed in the positions of the empty state maxima in the STM images. These two possibilities are illustrated in Fig. 7. The upper panel shows a row of Al dimers in the normal configuration. The lower panel shows the same row of Al dimers, but with each dimer rotated 90° so that it is parallel to the adjacent Si dimers. This parallel configuration might seem unlikely because of the strong bond angle distortions and the proximity of the metal atoms to atoms in the second subsurface layer of Si. However, an analogy can be drawn to the T_4 adsorption site for trivalent metals on the Si(111) surface, where a similar configuration has the lowest energy.¹¹ Furthermore, the parallel dimer configuration provides a natural explanation for the strict $2a$ periodicity observed along each row. It can always be argued that for the normal dimer orientation, it should be possible to insert additional dimers into a row to produce a one-unit-cell spacing analogous to that seen for Si or As on Si(100). This $1a$ periodicity is explicitly forbidden in the parallel dimer configuration. Further work is in progress to clarify the bonding site of the Al dimers on this surface.

The experimental work was carried out at Stanford University under the support of the Office of Naval Research. One of the authors (A.A.B.) acknowledges support from AT&T. J.N. acknowledges helpful comments from R. M. Feenstra.

¹J. Nogami, Sang-il Park, and C. F. Quate, *Appl. Phys. Lett.* **53**, 2086 (1988).

²A. A. Baski, J. Nogami, and C. F. Quate, *J. Vac. Sci. Technol. A* **8**, 245 (1990).

³A. A. Baski, J. Nogami, and C. F. Quate, *Phys. Rev. B* **43**, 9316 (1990).

⁴A. A. Baski, J. Nogami, and C. F. Quate, *J. Vac. Sci. Technol. A* (to be published).

⁵T. Ide, T. Nishimori, and T. Ichinokawa, *Surf. Sci.* **209**, 335 (1989).

⁶Inder P. Batra, *Phys. Rev. Lett.* **63**, 1704 (1989).

⁷J. Knall, J.-E. Sundgren, G. V. Hansson, and J. E. Greene, *Surf. Sci.* **166**, 512 (1986).

⁸B. Bourguignon, K. L. Carleton, and S. R. Leone, *Surf. Sci.* **204**, 455 (1988).

⁹B. Bourguignon, R. V. Smilgys, and S. R. Leone, *Surf. Sci.* **204**, 473 (1988).

¹⁰Sang-il Park and C. F. Quate, *Rev. Sci. Instrum.* **58**, 2010 (1987); commercial STM provided by Park Scientific Instruments, Mountain View, CA 94043.

¹¹John E. Northrup, *Phys. Rev. Lett.* **57**, 154 (1986).

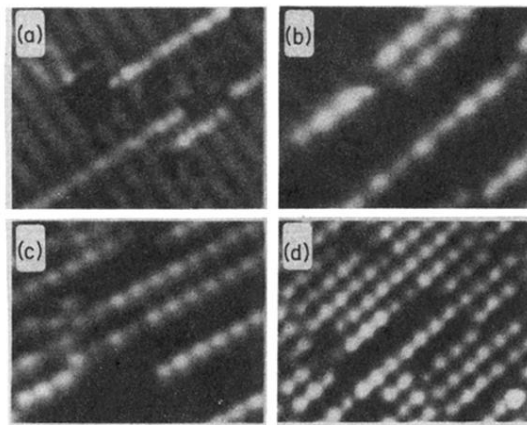


FIG. 2. Four images showing the coverage evolution of the surface below 0.5 ML of Al. The sequence of coverages is 0.1, 0.2, 0.25, and 0.4 ML for Figs. 2(a)–2(d), respectively. Figure 2(a) is a filled state image. The remaining three figures are empty state images.

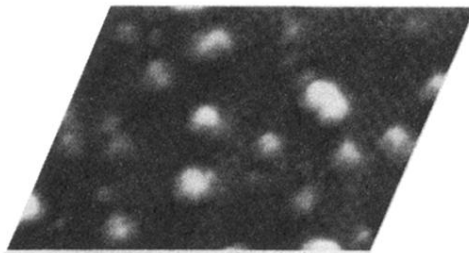


FIG. 4. An image of 0.6 ML of Al on the surface. The square array covering most of the surface is the 2×2 phase. Deposition of more than 0.5-ML Al results in the growth of Al clusters on the surface, which appear as bright irregular shapes in this topograph.

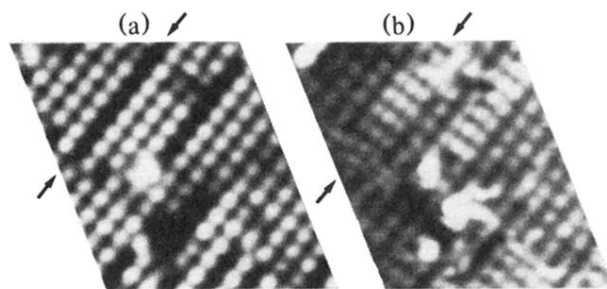


FIG. 5. A pair of images of the surface at 0.4 ML, taken in parallel at -2 -V and $+2$ -V tip bias, showing the (a) empty and the (b) filled states of the surface. A pair of arrows indicates a single row of 2×3 unit cells in both images.